

# The Distribution of Satellite Galaxies: The Great Pancake

Noam I Libeskind<sup>1</sup>, Carlos S Frenk<sup>1</sup>, Shaun Cole<sup>1</sup>, John C Helly<sup>1</sup>, Adrian Jenkins<sup>1</sup>,  
Julio F Navarro<sup>2</sup> and Chris Power<sup>3</sup>

<sup>1</sup>*Department of Physics, University of Durham, Science Laboratories, South Road, Durham, DH1 3LE, U.K.*

<sup>2</sup>*Department of Physics and Astronomy, University of Victoria, 3800 Finnerty Road, Victoria, BC V8P 1A1, Canada*

<sup>3</sup>*Centre for Astrophysics & Supercomputing, Swinburne University of Technology, P.O. Box 218, Hawthorn, Victoria 3122, Australia*

3 September 2018

## ABSTRACT

The 11 known satellite galaxies within 250 kpc of the Milky Way lie close to a great circle on the sky. We use high resolution N-body simulations of galactic dark matter halos to test if this remarkable property can be understood within the context of the cold dark matter cosmology. We construct halo merger trees from the simulations and use a semianalytic model to follow the formation of satellite galaxies. We find that in all 6 of our simulations, the 11 brightest satellites are indeed distributed along thin, disk-like structures analogous to that traced by the Milky Way’s satellites. This is in sharp contrast to the overall distributions of dark matter in the halo and of subhalos within it which, although triaxial, are not highly aspherical. We find that the spatial distribution of satellites is significantly different from that of the most massive subhalos but is similar to that of the subset of subhalos that had the most massive progenitors at earlier times. The elongated disk-like structure delineated by the satellites has its long axis aligned with the major axis of the dark matter halo. We interpret our results as reflecting the preferential infall of satellites along the spines of a few filaments of the cosmic web.

## 1 INTRODUCTION

In the cold dark matter (CDM) cosmology, structure builds up through fragments merging together in a roughly hierarchical way. High resolution N-body simulations of the formation of dark matter halos in the  $\Lambda$ CDM cosmology have demonstrated that the cores of tightly bound fragments often survive the merging process and remain as distinct substructures orbiting inside a parent halo (Klypin et al. 1999, Moore et al. 1999). The centre of the main halo and the accompanying substructures are naturally identified with the formation sites of central and satellite galaxies respectively. The N-body simulations suggest that the mass functions of surviving substructures in galactic and cluster halos are roughly self-similar. Yet, the luminosity function of galaxies in rich clusters has a very different shape from the luminosity function of satellites in smaller systems such as the Milky Way or the Local Group (Kauffmann et al. 1993; Mateo 1998; Trentham & Hodgkin 2002; Benson et al. 2002b). Not only is the central galaxy much more prominent in Milky-Way systems than in galaxy clusters, but the number of surviving subhalos in simulations of galaxy-sized halos far exceeds the number of the known satellites of the Milky Way.

The discrepancy between the small number of satellites around the Milky Way and the large number of surviving substructures, once regarded as a major challenge to the cold dark matter cosmology, is now thought to be due to the astrophysical processes that regulate the cooling of gas in halos

and its subsequent transformation into stars. The increase in the entropy of the intergalactic medium brought about by the reionization of the gas at early times has been identified as a possible solution to the so-called “satellite problem” (Kauffmann et al. 1993; Bullock 2002; Benson et al. 2002a; see also Stoehr et al. 2002). Reionization sharply reduces the efficiency of gas cooling in small halos so that galaxies that formed prior to reionization are preferentially those that end up as satellites in systems like the Local Group. The detailed model calculated by Benson et al. (2002a) which includes the effects of early reionization as well as other forms of feedback, reproduces many observed properties of the Local Group’s satellite system, including the distribution function of circular velocity, the luminosity function and the colour distribution.

While the original satellite problem is no longer deemed a serious challenge, another related potential problem for the cosmological paradigm has recently been highlighted by Kroupa, Thies & Boily (2005). These authors argue that the strongly flattened spatial distribution of the 11 brightest dwarf satellites of the Milky Way, a feature known, but not understood, for many years (Lynden-Bell 1982; Majewski 1994), is inconsistent with the  $\Lambda$ CDM model. According to Kroupa et al. (2005), CDM models predict a roughly isotropic distribution of satellites. They based this conclusion on the assumption that the spatial distribution of satellites resembles the spatial distribution of the halo dark matter which indeed, as N-body simulations have demon-

strated, is approximately (although not exactly) spherical (e.g. Frenk et al. 1988; Jing & Suto 2002; Bullock 2002).

In this paper, we demonstrate that the satellites of systems like the Local Group do *not* trace the distribution of halo mass. On the contrary, the satellites in our suite of high resolution N-body simulations are generally arranged in highly flattened configurations which have similar properties to those of the Milky Way satellite system. This, at first sight surprising, result is a reflection of the anisotropic accretion of subhalos which generally stream into the main halo along the filaments of the cosmic web. The flattened structure in which the Milky Way satellites lie traces a great circle on the sky and is approximately perpendicular to the Galactic Plane. In our simulations, the satellite structures tend to be aligned with the major axis of the triaxial halo mass distribution, that is, the longest axis of the halo is close to lying in the principal plane of the satellite distribution.

As this paper was nearing completion, two related papers appeared on astro-ph. Both of them used high-resolution simulations of galaxy halos similar to those that we have performed. Kang et al. (2005) identified “satellites” in their 4 simulations with randomly chosen dark matter particles taken either from the halo as a whole or exclusively from substructures. They were able to find flattened satellite systems similar to that of the Milky Way in the former case but not in the latter. Zentner et al. (2005) found satellites in three N-body simulations of Milky-Way type systems also in two different ways. In the first, they used the semi-analytic model of Kravtsov, Gnedin & Klypin (2004) which is based on similar principles as those applied by Benson et al. (2002a). In their second model, they identified satellites with the most massive subhalos. Zentner et al. (2005) found that in both cases, the satellite systems had a planar distribution similar to that in the Milky Way and argued that the degree of central concentration of the satellite systems plays an important role in this result. They also showed that the population of subhalos as a whole is anisotropic and preferentially aligned with the major axis of the triaxial halo.

Like Zentner et al. (2005), our study employs a semi-analytic model to follow the formation of the visible satellites. In this respect, both these studies are quite different from that of Kang et al. (2005) who based their conclusions purely on dark matter particles. Our model differs from that of Zentner et al. (2005) in several important respects. Our simulation codes and methods for identifying substructure are different. While they considered three halos specifically chosen to lie on a filament, we used 6 simulations randomly chosen from a large cosmological volume. The biggest difference, however, concerns the semi-analytic models used in the two studies. While both of them give a reasonable match to several observed properties of the Milky Way’s satellites, our semi-analytic model has been applied and tested much more extensively than that of Kravtsov et al. (2004). The model we use is based on the GALFORM code of Cole et al. (2000) as extended by Benson et al. (2002b). This model has been shown to give an acceptable account of many properties of the galaxy population as a whole including the luminosity function in various passbands, from the UV to the far infrared, and in various environments, distributions of colour, size and morphological type, etc. The model is also relatively successful at matching the properties of galaxies at

	$N_{\text{tot}}$ ( $10^6$ )	$N_{\text{hr}}$ ( $10^6$ )	$R_{\text{vir}}$ ( $h^{-1}$ kpc)	$N_{\text{vir}}$ ( $10^6$ )
gh1	14.6	12.9	110	1.07
gh2	18.1	16.2	131	1.74
gh3	18.0	16.2	170	3.73
gh6	25.5	22.2	169	3.76
gh7	19.2	17.3	156	2.99
gh10	13.4	12.1	133	1.86

**Table 1.** Parameters for the six  $N$ -body halo simulations. For each halo (column 1), (2) shows the total number of particles in the simulation box, (3) the number of high resolution particles in the simulation, (4) the virial radius of the halo in  $h^{-1}$  kpc defined as the distance from the centre at which the mean interior density is  $178\rho_{\text{crit}}$ , and (5) the number of particles inside the virial radius. In all cases, the simulation cube has co-moving length of  $35.325 h^{-1}\text{Mpc}$ , and the mass of the high resolution particles is  $2.64 \times 10^5 h^{-1}M_{\odot}$ .

high-redshift, as discussed in Baugh et al. (2004). Finally, the two studies use somewhat different methods to quantify the distribution of Milky Way satellites and to compare the results with the observations. On the whole, the conclusions of the two studies are consistent although there remain some differences as we discuss in Section 4.

The remainder of this paper is organised as follows: in Section 2 we outline the methods used; in Section 3.1 we present our results which we interpret in Section 3.2; in Section 4 we discuss the implications of our findings.

## 2 SIMULATIONS AND GALAXY FORMATION MODEL

We have analyzed 6 high-resolution  $N$ -body simulations of galactic-size dark matter halos carried out with the GADGET code (Springel et al. 2001a). The halos, chosen to have a mass  $\sim 10^{12}M_{\odot}$ , were otherwise randomly selected from a large cosmological simulation of a cubic region of side  $35.325 h^{-1}$  in a flat  $\Lambda\text{CDM}$  universe (with  $\Omega_{\text{m}} = 0.3$ ,  $h = 0.7$ ,  $\sigma_8 = 0.9$ ). The simulation was executed a second time adding “high resolution” (i.e. small mass) particles, and appropriate small scale power in the initial conditions, to a region surrounding the halo under consideration. These simulations have been studied extensively in previous papers (Power et al. 2003, Hayashi et al. 2004, Navarro et al. 2004) and we refer the reader to those papers for specific details of how the simulations were carried out. Table 1 summarizes the important parameters of the simulations.

We identified bound substructures in the simulation using the algorithm SUBFIND (Springel et al. 2001b). First, “friends-of-friends” groups (Davis et al. 1985) are found by linking together particles whose separation is less than 0.2 times the mean interparticle separation, corresponding roughly to particles within the virialized region of the halo. SUBFIND then identifies substructures within these halos based on an excursion set approach, using the spatial and velocity information for each particle in order to define self-bound objects.

For each halo, we generate a complete merger history, identifying all progenitor and descendant halos, as described

in Helly et al. (2003). The semi-analytic galaxy formation model is calculated along each branch of the merger tree. This is based on the model described in detail in Cole et al. (2000) and Benson et al. (2002b). The model includes the following physical processes: (i) the shock-heating and virialization of gas within the gravitational potential well of each halo; (ii) radiative cooling of gas onto a galactic disk; (iii) the formation of stars from the cooled gas; (iv) the effects of photoionization on the thermal state and cooling properties of the intergalactic medium; (v) reheating and expulsion of cooled gas through feedback processes associated with stellar winds and supernovae explosions (see Benson et al. 2003b); (vi) the evolution of the stellar populations; (vii) the effects of dust absorption and radiation; (viii) the chemical evolution of the stars and gas; (ix) galaxy mergers (which, depending on the violence of the merger, may be accompanied by starbursts and the formation of a bulge – see Baugh et al. 2004); (x) the evolution of the size of the disk and bulge.

Our model differs from that of Cole et al. (2000) and Helly et al. (2003) in the way in which galaxy mergers are treated. In the current model, the positions of satellite galaxies and the time when they merge is determined by using information from SUBFIND. Central galaxies are placed on the most bound particle of the most massive subgroup in the halo. (SUBFIND identifies the background mass distribution of the halo as a separate subgroup, so this is generally a robust way to define the centre of the halo.) Satellite galaxies are placed on the descendant subhalo of the progenitor halo in which they formed. If the subhalo ceases to be identified by SUBFIND at some later output time, we continue to trace its constituent particles and place the galaxy at the centre of mass of this group of particles. A galaxy is considered to have merged onto the central galaxy if its distance from the central galaxy is less than the spatial extent of the set of particles it is associated with.

An overview of the results of our semianalytic model as regards the evolution of the galaxy population as a whole may be found in Benson et al. (2003a) and Baugh et al. (2004) while results relevant to the satellites of the Milky Way may be found in Benson et al. (2002a).

### 3 RESULTS

We begin by quantifying the shapes of dark matter halos in the simulations and sub-systems within them. We then interpret the results in terms of the formation histories of the halos and their subsystems.

#### 3.1 The morphology of halos and their subsystems

The semianalytic model applied to the N-body simulations provides the position and internal properties of the central galaxy in each halo and its satellites. According to the semi-analytic model, three of the central galaxies are spirals and three ellipticals. For the purpose of comparing with the analysis of Kroupa et al. (2005), we select the 11 most massive satellites in each halo within a distance of 250 kpc from the central galaxy. We calculate the moment of inertia tensor of this satellite subsample, weighting each object equally, and obtain the principal axes of the distributions.

Fig. 1 shows three orthogonal projections along the

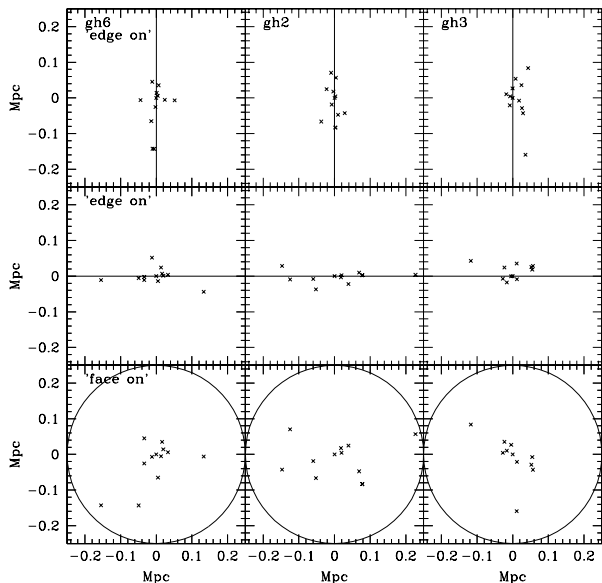


**Figure 1.** Projections of the positions of the 11 most massive satellites within 250 kpc of the central galaxy along the principal axes of the inertia tensor in simulations gh6, gh2 and gh3.

principal axes of the satellite systems in three of our six simulations. The other three are very similar. The figure reveals, remarkably, that the loci of the 11 most massive satellites define a thin, disk-like structure around the central galaxy. As we show below, in most cases, the satellite structure is aligned with the major axis of its triaxial host dark matter halo.

The distribution of the visible satellites differs significantly from the distribution of the dark matter substructures identified by SUBFIND. Fig. 2 is analogous to Fig. 1 but the points plotted now correspond to the most massive 200 substructures found within 250 kpc of the central galaxy. The projections are along the principal axes of the inertia tensor of the substructure systems. It is evident that the distribution of substructures is much less anisotropic than that of the satellites in Fig. 1.

The eigenvalues of the diagonalized inertia tensor are proportional to the rms deviation of the  $x$ ,  $y$  and  $z$  coordinates relative to the principal axes. Denoting the major, intermediate and minor axes by  $a$ ,  $b$  and  $c$  respectively ( $a > b > c$ ), the flattening of the system may be quantified by the ratios  $c/a$  and  $b/a$ . The early N-body simulations of Frenk et al. (1988) showed that CDM halos are triaxial and recent work indicates that  $c/a = 0.7 \pm 0.17$ , and  $b/a > 0.7$  (Bullock 2002).

The axial ratios, found by diagonalizing the moment of inertia tensor, of the dark matter halos and various sub-systems of objects within them are plotted Fig. 3. Fig. 3a shows that our simulated halos have axial ratios consistent with those found in previous simulations and tend to congregate near the top right of the panel corresponding to nearly spherical objects. With the exception of an outlier, gh6, which is significantly prolate, this is also the region populated by the massive subhalos.

The axial ratios of the systems consisting of the 11 most

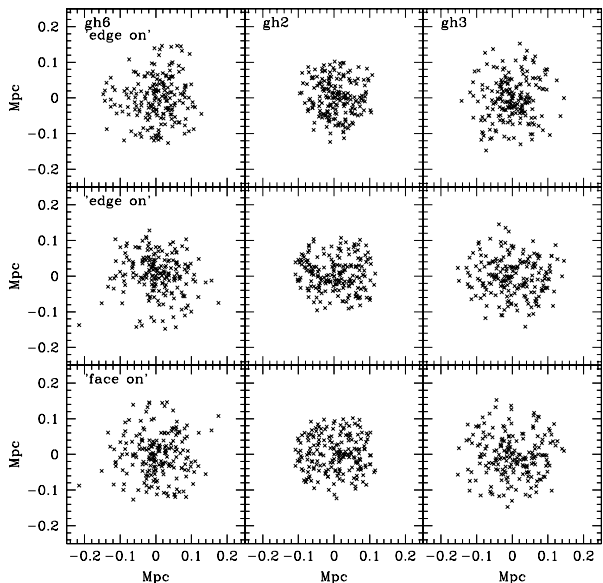


**Figure 2.** Projections of the positions of the 200 most massive dark matter substructures within 250 kpc of the central galaxy along the principal axes of the inertia tensor in simulations gh6, gh2, and gh3.

massive visible satellites are plotted in Fig. 3b. The triangles correspond to our full semianalytic model and the squares to a variant in which the early reionization of the intergalactic medium is not included. The satellite systems in the two models have similar flattening because more than 80 % of the subhalos that host the brightest satellites in the two cases are the same. However, as discussed by Benson et al. (2002a), neglecting the effects of reionization leads to an overprediction of the number of faint galaxies, including satellites in the Milky Way. Whether reionization is included or not, the satellites in our simulations cluster around the location of the Milky Way data marked by a cross in Fig. 3b. This is the main result of our analysis: the flattening of the satellite system in our simulations is in excellent agreement with that of the Milky Way satellite system.

It is clear from Fig. 3a and Fig. 3b that the most massive visible satellites inhabit a biased subset of subhalos. To explore the origin of this bias, we select two subsets of subhalos: the 11 most massive subhalos at  $z = 0$  and the 11 subhalos which had the most massive progenitors prior to being incorporated within the virial radius of the main halo. The flattening of these two systems is compared in Fig. 3c. The figure shows that the crucial factor in establishing a highly flattened system *is not* the final mass of the subhalo but *the mass of the largest progenitor*. It is the latter that correlates well with the final stellar mass or luminosity of the visible satellite, as shown in Fig. 4a. Here we plot the stellar mass of each satellite galaxy against the mass of its largest progenitor. This strong correlation is a result if the GALFORM model readily making the most luminous galaxies in the most massive progenitor halos. In contrast, Fig. 4b shows there is no correlation between the stellar mass of each satellite and the mass of its host substructure. This is due

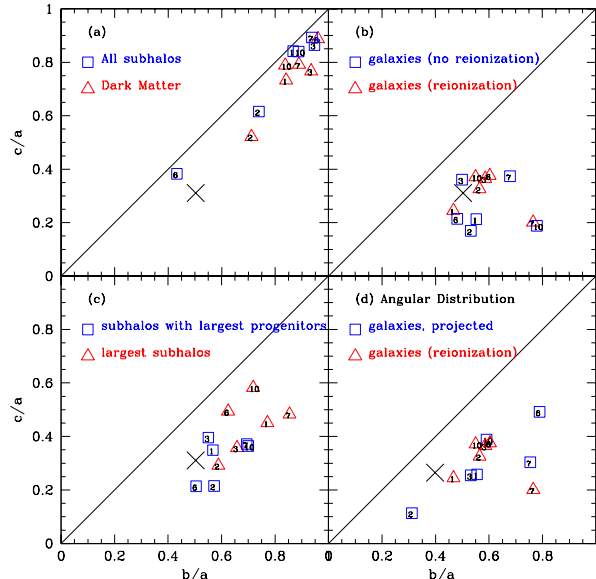


**Figure 3.** Minor to major ( $c/a$ ) versus intermediate to major ( $b/a$ ) axial ratios. Since  $a > b > c$ , the upper left triangular half of this plot cannot contain any points. Along the diagonal lie prolate objects and along the right vertical axis lie oblate objects. The numbers inside each symbol identify the simulated halo. The 'X' indicates the axial ratios of the Milky Way's satellite system from Kroupa et al. 2005. Only data out to a radius of 250 kpc is used in all cases. Panel (a) compares the axial ratios of the dark matter halos (triangles) with those of the system consisting of the dark matter substructures (squares). Panel (b) compares the axial ratios of the systems made up of the 11 most massive visible galaxies in models with and without early reionization (triangles and squares respectively). Panel (c) compares the axial ratios of the systems of 11 most massive substructures with those of the systems consisting of the 11 substructures that had the most massive progenitors. Panel (d) compares the axial ratios of the systems made up of the 11 most massive visible satellites in our full model (triangles) with those of the same systems but with the radial distances of each satellite normalized to a common value. This same operation is performed on the Milky Way data and so the Kroupa et al. 2005 point moves slightly

to the subhalos having been subjected to various amounts of tidal stripping.

Comparison of Fig. 3a and Fig. 3c indicates that the flattening of the systems consisting of the 11 most massive visible satellites and the 11 subhalos that had the most massive progenitors are very similar. This is an important result because it demonstrates that our main conclusion regarding the compatibility of the Kroupa et al. (2005) data with the CDM cosmology does not depend on the details of our semianalytic modelling of galaxy formation. So long as the brightest satellites form in those subhalos with the most massive progenitors, our conclusions stand.

With only 11 satellites in our main samples, the possibility that our estimate of the moments of inertia might be biased by the presence of outliers is a concern. We investigate the sensitivity of our results to outliers by scaling all radial positions to a common value while keeping the angles of each radius vector fixed. The axial ratios of the rescaled

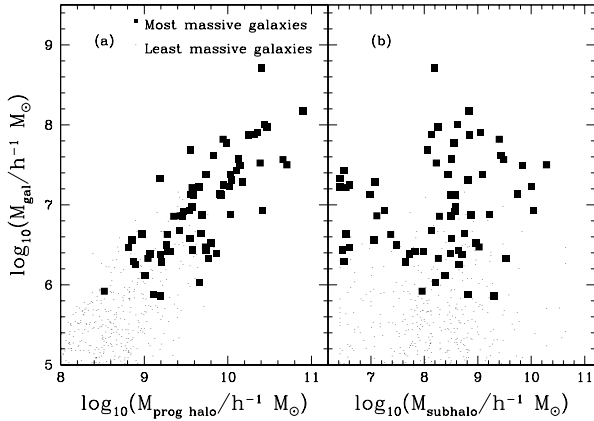


**Figure 4.** (a) Stellar mass in each satellite galaxy as a function of the mass that its largest progenitor halo had before becoming incorporated into the main halo. (b) Stellar mass in each satellite galaxy as a function of the mass of the substructure the galaxy currently resides in. The squares show results for the 11 most massive satellites in all 6 simulations, while the dots show results for the less massive satellites. The overlap in panel (a) is largely due to the smallest satellite mass varying between simulations

data are compared to the axial ratios of the 11 most massive satellites in Fig. 3d. Rescaling the satellite radial distances scatters our estimates of axial ratios somewhat but does not, on average, lower the overall flattening of the systems. As shown in the figure, rescaling the Milky Way data in the same way also has a small effect on the axial ratios.

Finally, we consider the connection between the highly anisotropic distribution of satellites and the orientation of their host dark matter halo. Consider the vector pointing along the major axis of the distribution (i.e. along  $a_{\text{sat}}$ ). Let  $\theta$  denote the angle between this vector and a vector pointing along the major axis of the halo,  $a_{\text{DM}}$ . For our six simulations, we find that  $\cos(\theta)$  equals to 0.768, 0.979, 0.702, 0.747, 0.387, 0.942 for galaxy halos gh1, gh2, gh3, gh6, gh7 and gh10 respectively. Thus, apart from gh7, there is a very strong alignment between the major axis of the disk-like satellite systems and the major axis of the parent dark matter halo. In the Milky Way, the major axis of the satellite disk-like structure is perpendicular to the galactic disk. Thus, if our galaxy resides in a dark matter halo similar to those that we have simulated, then the disk must be aligned such that its normal vector points in the direction of the halo major axis. Interestingly, this is exactly the alignment observed in recent gasdynamical simulations of the formation of spiral galaxies by Navarro, Abadi & Steinmetz (2004).

### 3.2 Interpretation

The highly anisotropic distribution of satellite galaxies in Milky Way type systems is a somewhat surprising outcome of galaxy formation in a CDM universe. This is particularly so in view of the fact that the population of subhalos as a whole is much less anisotropic and has axial ratios similar to those of the halo dark matter. The key to understanding the origin of the anisotropic satellite distribution lies in the connection between halos and the cosmic web and, in particular, in the way in which satellites are accreted onto

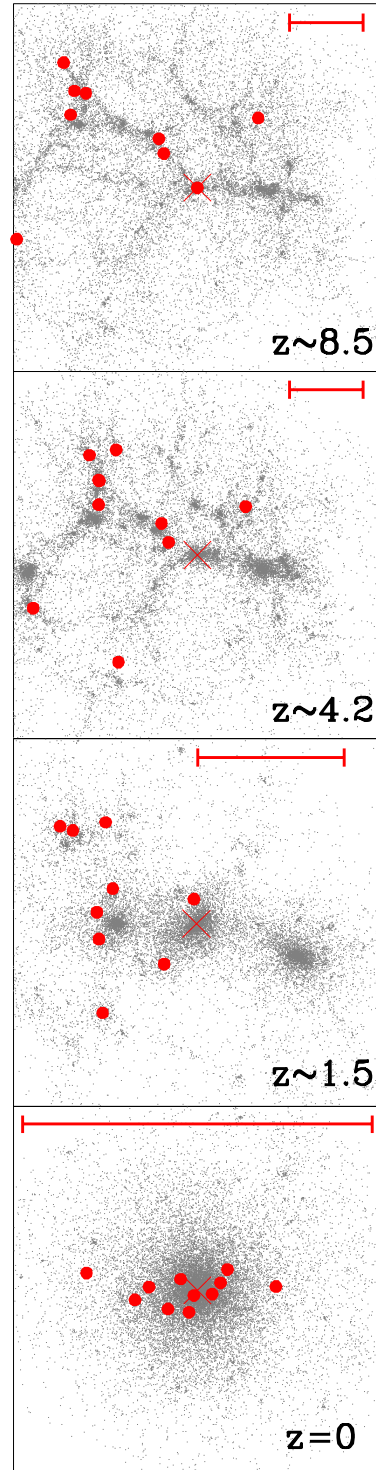


**Figure 5.** The formation of a galactic halo and its satellites. The points show a random 1% of the dark matter particles that end up in the main halo and the red circles the positions of the 11 most massive satellites that end within 250 kpc of the main galaxy by the present day. The scale of each plot is indicated by the red line which has a co-moving length of 400 kpc. The initial collapse produces a 2D structure – a large pancake of dark matter.

the main halo. Fig. 5 illustrates the anisotropic nature of satellite accretion. The dots show a random 1% of the dark matter particles that end up in the main halo at the final time. The red circles mark the locations of the most massive progenitors of the 11 satellites that have the largest stellar mass at the final time. Rather than originating isotropically, those halos destined to become bright visible satellites are accreted primarily along one or two of the cosmic web filaments.

The first panel in the figure illustrates the highly anisotropic collapse typical of CDM structures on galactic scales. Careful inspection of the time evolution of the system shows that the collapse occurs first along 2D sheet-like structures which subsequently wrap up into filamentary streams of dark matter. By  $z \sim 4.2$ , these filamentary “highways” along which proto-satellite galaxies form are well established. The filaments are generally thicker than the locus of the largest proto-galactic halos which tend to concentrate towards the central, densest parts of the filament in a near 1-dimensional configuration. As the most massive halo progenitors collapse to form the main galaxy, this alignment is largely preserved. Smaller halos are more widely scattered across the thick filaments, reflecting their weaker clustering strength (Cole & Kaiser 1989; Mo, Mao, & White 1999). In addition, they are often accreted over a longer period and from a larger range of directions. Their distribution, now lacking a preferred orientation, ends up being much less anisotropic than that of the most massive halos. Whether reionization is included or not, satellite galaxies in the semi-analytic model form preferentially in the subhalos with the most massive progenitors and thus inherit their highly flattened configuration.

#### 4 DISCUSSION AND CONCLUSIONS

We have shown that the, at first sight surprising, flattened distribution of satellites in the Milky Way is the natural outcome of the anisotropic accretion of matter along a small number of filaments, characteristic of halo formation in the CDM cosmology. Kroupa et al. (2005) reached the opposite conclusion, that the observed satellite distribution is incompatible with the CDM model, because they neglected the fact that the satellites do not trace the distribution of halo dark matter but form instead in the most massive halos whose spatial distribution is biased.

Our results are not directly comparable to those of Kang et al. (2005) who also attempted to interpret the flattened distribution of Milky Way satellites with the aid of high-resolution N-body simulations. Kang et al. (2005) assumed that the satellites follow the dark matter distribution in the halo and did not consider the formation sites of satellites in detail. Zentner et al. (2005), on the other hand, implemented a semi-analytic model similar to ours in N-body simulations also similar to ours and those of Kang et al. (2005).

Our results are broadly consistent with those of Zentner et al. (2005). Unlike them, we did not choose halos specifically lying along filaments but selected them at random from a large cosmological simulation. In the event, three of our halos would, according to our semianalytic model, host spiral galaxies and the other three elliptical galaxies.

One difference between the two studies is that Zentner et al. (2005) found an acceptable match to the Milky Way satellite distribution both in their semianalytic model and in a model in which the satellites are identified with the most massive subhalos at the final time. We have shown that the distribution of the latter is not as flattened as the distribution of Milky Way satellites. The crucial factor is not the final mass of the halo which is affected by tidal stripping, but the mass of the largest progenitor before it is accreted into the main halo. Indeed, if the satellites are identified with the halos that had the largest progenitors, then their flattened distribution is very similar to that of the satellites identified by our semianalytic model. Thus, our conclusions are independent of the details of our galaxy formation modelling.

As was also found by Zentner et al. (2005), the major axis of the flattened satellite distribution in our simulations points close to the direction of the major axis of the parent halo. This alignment reflects the preferential accretion of mass onto the halo along the dominant filament. An important consequence of this result is that if the Milky Way resembles the systems we have simulated, then the Galactic disk should lie in the plane perpendicular to the major axis of the halo because the observed satellite system itself is perpendicular to the Galactic disk. Interestingly, this is exactly the configuration found in the recent gasdynamical simulations of spiral galaxy formation by Navarro, Abadi & Steinmetz (2004).

The satellite alignment that we have found in our simulations is almost certainly related to the “Holmberg effect,” (Holmberg 1969) the observation that the satellites of external galaxies within a projected radius of  $r_p \sim 50$  kpc tend to lie preferentially in a cone along the galaxies’ minor axis, avoiding the equatorial regions. To test this observation requires a larger number of simulations than those we have performed. Similarly, our current simulations are inadequate to test the extension of the Holmberg effect uncovered by Zaritsky et al. (1997) from a study of isolated spirals which also revealed an excess of satellites along the minor axis of the galaxy, now out to projected distances of  $r_p \sim 500$  kpc. A similar result was found by Sales & Lambas (2004) from a much larger sample of galaxies drawn from the 2 degree field galaxy redshift survey. They too found an anisotropic distribution for  $r_p < 500$  kpc, but only for satellites moving with a velocity relative to their host of  $\Delta v < 160$  km s<sup>-1</sup>. In contrast, Brainerd (2004) found the opposite effect in a sample of satellites from the Sloan Digital Sky Survey, an alignment along the major axis at small radii ( $r_p < 100$  kpc) and an isotropic distribution beyond.

Although our simulations are not large enough to study the distribution of satellites beyond the inner 250 kpc of the galactic centre, it seems likely that the anisotropic distribution of satellites will continue out to larger separations. We intend to study this problem in a larger set of simulations.

In summary, we have found that flattened distribution of the Milky Way satellites, first noted by Lynden-Bell (1982), and most recently highlighted by Kroupa et al. (2005), turns out to have a simple explanation in the context of structure formation in the CDM model. It is merely a reflection of the intimate connection between galactic dark matter halos and the cosmic web.

## REFERENCES

- Baugh C., Lacey C. G., Frenk C. S., Benson A. J., Cole S., Granato G. L., Silvia L., Bressan A., 2004, *New A R*, 48, 1239
- Benson A. J., Frenk C. S., Lacey C. G., Baugh C. M., Cole S., 2002a, *MNRAS*, 333, 177
- Benson A. J., Lacey C. G., Baugh C. M., Cole S., Frenk C. S., 2002b, *MNRAS*, 333, 156
- Benson A. J., Bower R. G., Frenk C. S., Lacey C. G., Baugh C. M., Cole S. 2003a, *ApJ*, 599, 38
- Benson A. J., Frenk C. S., Baugh C. M., Cole S., Lacey C. G., 2003b, *MNRAS*, 343, 679
- Brainerd T., *ApJL*, in press (astro-ph/0408559)
- Bullock J. S., Kravtsov A. V., Weinberg D. H., 2000, *ApJ*, 539, 517
- Bullock, J. S. astro-ph/0106380
- Cole S., Kaiser N., 1989, *MNRAS*, 237, 1127
- Cole S., Lacey C. G., Baugh C. M., Frenk C. S., 2000, *MNRAS*, 319, 168
- Combes F., *New A R*, 46, 755 (astro-ph/0206126)
- Davis M., Efstathiou G., Frenk C. S., White S. D. M., 1985, *ApJ*, 292, 371
- Frenk C. S., White S. D. M., Davis M., Efstathiou G., 1988, *ApJ*, 327, 507
- Hayashi E., Navarro J. F., Power C., Jenkins A., Frenk C. S., White S. D. M., Springel V., Stadel J., Quinn T., 2004, *MNRAS*, 355, 794
- Helly J., Cole S., Frenk C. S., Baugh C. M., Benson A., Lacey C. G., 2003, *MNRAS*, 338, 903
- Holmberg E., 1969, *Ark. Astron.*, 5, 305
- Jing Y. P., Suto Y., 2002, *ApJ*, 574, 538
- Kang X., Mao S., Gao L., Jing Y. P., *A&A* submitted (astro-ph/0501333)
- Kauffmann G., White S. D. M., Guiderdoni B., 1993, *MNRAS*, 264, 201
- Klypin A., Kravtsov A. V., Valenzuela O., Prada F., 1999, *ApJ*, 522, 82
- Kravtsov A. V., Gnedin O., Klypin A. A., 2004, *ApJ*, 609, 482
- Kroupa P., Thies C., Boily C. M., 2005, *A&A*, 431, 517 (astro-ph/0410421)
- Lynden-Bell D., 1982, *Obs.*, 102, 202
- Majewski S. R., 1994, *ApJL*, 431, L17
- Mateo M. L., 1998, *ARA&A*, 36, 435
- Mo H. J., Mao S., White S. D. M., 1999, *MNRAS*, 304, 175
- Moore B., Ghigna S., Governato F., Lake G., Quinn T., Stadel J., Tozzi P., 1999, *ApJ*, 524, L19
- Moore B., Kazantzidis S., Diemand J., Stadel J., 2004, *MNRAS*, 354, 522
- Navarro J. F., Hayashi E., Power C., Jenkins A., Frenk C. S., White S. D. M., Springel V., Stadel J., Quinn T., 2004, *MNRAS*, 349, 1039
- Navarro J. F., Abadi M. G., Steinmetz M., 2004, *ApJL*, 613, L41
- Power C., Navarro J. F., Frenk C. S., Jenkins A., White S. D. M., Springel V., Stadel J., Quinn T., 2003, *MNRAS*, 338, 14
- Sales L., Lambas D., 2004, *MNRAS*, 348, 1236
- Springel V., White S. D. M., Tormen G., Kauffmann G., 2001b, *MNRAS*, 328, 726
- Springel V., Yoshida N., White S. D. M., 2001a, *New Astronomy*, 6, 51
- Stoehr F., White S. D. M., Tormen G., Springel V., 2002, *MNRAS*, 335, L84
- Susa H., Umemura M., 2004, *ApJ*, 600, 1
- Trentham N., Hodgkin S., 2002, *MNRAS*, 333, 423
- White S. D. M., Rees M. J., 1978, *MNRAS*, 183, 341
- Zaritsky D., Smith R., Frenk C., White S. D. M., 1997, *ApJ*, 478, L53
- Zentner A. R., Kravtsov A. V., Gnedin O. Y., Klypin A. A., *ApJ* submitted (astro-ph/0502496)